

March 27, 2022

## Compatibility of neutrino DIS data and global analyses of parton distribution functions

Hannu Paukkunen<sup>1</sup> and Carlos A. Salgado<sup>2</sup>

Departamento de Física de Partículas and IGFAE, Universidade de Santiago de Compostela, Galicia–Spain

### Abstract

Neutrino\antineutrino deep inelastic scattering (DIS) data provide useful constraints for the flavor decomposition in global fits of parton distribution functions (PDF). The smallness of the cross-sections requires the use of nuclear targets in the experimental setup. Understanding the nuclear corrections is, for this reason, of utmost importance for a precise determination of the PDFs. Here, we explore the nuclear effects in the neutrino\antineutrino-nucleon DIS by comparing the NuTeV, CDHSW, and CHORUS cross-sections to the predictions derived from the latest parton distribution functions and their nuclear modifications. We obtain a good description of these data and find no apparent disagreement between the nuclear effects in neutrino DIS and those in charged lepton DIS. These results also indicate that further improvements in the knowledge of the nuclear PDFs could be obtained by a more extensive use of these sets of neutrino data.

---

<sup>1</sup>hannu.paukkunen@usc.es

<sup>2</sup>carlos.salgado@usc.es

# 1 Introduction

The undisputed success of the recent global analyses of the free nucleon parton distribution functions (PDFs) [1, 2, 3] have proven the QCD factorization theorem as a well-working tool to analyse and interpret the experimental cross-sections measured at high-energy colliders. These analyses look for a universal set of PDFs,  $f_i^A(x, Q^2)$ , facilitating the cross-sections computations schematically as

$$\sigma_{AB \rightarrow h+X} = \sum_{i,j} f_i^A(Q^2) \otimes f_j^B(Q^2) \otimes \hat{\sigma}_{ij \rightarrow h+X}, \quad (1)$$

where  $\hat{\sigma}_{ij \rightarrow h+X}$  are perturbatively computable coefficients.

The usual procedure to obtain a global fit of PDFs is well established<sup>1</sup>: a functional form with  $N$  parameters is assumed for the different PDFs at a given initial scale  $Q_0^2$ . This initial condition is then evolved by the Dokshitzer-Gribov-Lipatov-Altarelli-Parisi (DGLAP) equations [4] and the best set of parameters obtained in an iterative procedure involving a quality criterion — a particular definition of the goodness of the fit through a generalized  $\chi^2$ . Several differences among the analyses, like the choice of the initial conditions, the choice of the data sets, the actual definition of the  $\chi^2$  or the approximations in the computation of the actual cross-sections, result in differences in the obtained PDFs. In particular, the neutrino\antineutrino DIS data is included only in part of these analyses due to the difficulty in removing the nuclear effects in a model-independent manner. These data are, however, of importance for the flavor decomposition of the PDFs which, on the other hand, affects the precision in the calculation of relevant cross-sections in present accelerators, in particular the LHC.

In the situation, where the nucleons are part of a bound nucleus, the factorization theorem could be theoretically more doubtful, as other processes like multiple scattering could ruin its applicability. However, the corresponding global analyses [5, 6, 7, 8] show also an excellent description of charged-lepton deep inelastic scattering (DIS) and Drell-Yan (DY) dilepton production data involving nuclear targets with the assumption of universal, process-independent, nuclear PDFs (nPDFs). This universality has also been checked in other processes, as single-inclusive hadron production in dAu collisions at RHIC, first introduced in [9] and then also in [5]. The access to harder and harder probes in nuclear collisions made the need of this type of analyses, and the corresponding checks of Eq. (1), also of utmost importance for the phenomenological interpretation of the imminent LHC heavy-ion program.

The amount of experimental information used in global nPDF fits is much smaller than the corresponding one for the free proton case. The total number of data points is  $\mathcal{O}(1000)$  scanning the range of  $x \gtrsim 10^{-2}$  in the perturbative region for different nuclei. These data are normally given in terms of the ratio of nuclear over free proton cross-sections (with the appropriate normalization factor) so most of the global analyses study the corresponding ratios of PDFs  $R_i^A(x, Q^2) \equiv f_i^{\text{bound}}(x, Q^2)/f_i^{\text{free}}(x, Q^2)$ . In

---

<sup>1</sup>A new approach with a different treatment of the initial conditions, especially designed to propagate experimental errors, has been recently proposed [3].

other words, the benchmarking role of the proton (or deuteron) cross-section in the experimental data is played in the global fits by a known set of free proton PDFs.

On the other hand, the abundant neutrino DIS data available for nuclear targets, both iron and lead, could provide strong constraints to the global fits of nuclear PDFs. The absence of a corresponding proton benchmarking data in this case indicates, however, that the price to pay is a modification of the usual procedure to check the compatibility among the different data sets within a DGLAP analysis. Several attempts to study nuclear effects in neutrino DIS exist [10, 11, 12, 13, 14]. It has been recently pointed out [14], that the NuTeV neutrino-Iron DIS data [15] displays a behaviour that hints to a possible disagreement between the nuclear modifications  $R_i^A(x, Q^2)$  in neutrino DIS, and those extracted from charged lepton DIS and DY process. If true, this would seriously doubt the validity of QCD factorization for bound nucleons. This is not only a problem for the nuclear PDF analyses, but would also make these data not suitable to be included in free proton global fits, and relevant constraints for different flavors would be lost.

In this work we address this issue by studying at the same time the compatibility of neutrino DIS data on iron and lead targets from three experiments within the approach of factorizable universal PDFs. These PDFs are taken from the latest available sets CTEQ6.6 [1] for protons and EPS09 [5] for nuclei, in which these data have not been included. We use, in particular, data from three collaborations NuTeV [15], CDHSW [16], and CHORUS [17]. The error analyses performed for PDFs allow us to propagate the uncertainties from other sets of data and to check the compatibility both between data and theory and among different sets of experimental data. In order to present the data in a more transparent manner, we provide as benchmark cross-sections for the nuclear case the ones computed theoretically using the known set of free proton PDFs. Our analysis finds a good description of neutrino DIS with nPDFs fitted to other data sets and do not find support for a breaking of the universality of the nuclear PDFs. We also comment on the compatibility between different data sets, in particular concerning the systematics in energy of the  $x$ -dependence in NuTeV data.

## 2 Framework

### 2.1 Computation Framework

A general expression for the differential DIS cross-sections can be written down in terms of three nuclear structure functions  $F_i^{\nu A, \bar{\nu} A}$  as

$$\frac{d^2\sigma^{\nu A, \bar{\nu} A}}{dxdy} = \frac{G_F^2 M_W^4}{(Q^2 + M_W^2)^2} \frac{ME_\nu}{\pi} \left[ xy^2 F_1^{\nu A, \bar{\nu} A} + \left(1 - y - \frac{xyM}{2E_\nu}\right) F_2^{\nu A, \bar{\nu} A} \pm xy \left(1 - \frac{y}{2}\right) F_3^{\nu A, \bar{\nu} A} \right]. \quad (2)$$

where  $y = Q^2/(2xME_\nu)$ ,  $G_F = 1.16637 \times 10^5 \text{ GeV}^2$  is the Fermi constant,  $M = 0.938 \text{ GeV}$  denotes the nucleon mass,  $M_W = 80.398 \text{ GeV}$  the mass of the  $W$  boson, and  $E_\nu$  to the neutrino energy. The “+” sign in front of the last term refers to the neutrino induced process, whereas “−” sign corresponds to the antineutrino scattering.

Each of the nuclear structure functions are composed of those of the bound protons and neutrons

$$F_i^A = \frac{Z}{A} F_i^{\text{proton},A} + \frac{A-Z}{A} F_i^{\text{neutron},A}. \quad (3)$$

We calculate the structure functions in the next-to-leading order QCD-improved parton model, schematically as a convolution between the perturbative Wilson coefficients  $\omega$  and the PDFs  $f_k^{\text{proton},A}$

$$F_i^{\text{proton},A} = \sum_k \omega_{ik} \otimes f_k^{\text{proton},A}, \quad (4)$$

where the  $k$  runs over all parton flavors. The neutron structure functions  $F_i^{\text{neutron},A}$  are computed correspondingly by assuming the isospin symmetry, i.e.

$$f_u^{\text{neutron},A} = f_d^{\text{proton},A}, \quad f_d^{\text{neutron},A} = f_u^{\text{proton},A}. \quad (5)$$

The effects of the heavy quarks are taken into account by the SACOT-prescription [18, 19, 20, 21, 22]. This is also the scheme which was adopted by CTEQ6.6 [1] analysis. This set will be used here to compute the benchmark cross-sections for the neutrino-nucleon cross-sections.

The nuclear modifications to the free proton PDFs  $f_k^{\text{proton}} = f_k^{\text{CTEQ6.6}}$  are taken from the recent EPS09-analysis<sup>2</sup> [5], which relates the nuclear PDFs to the free proton ones by a multiplicative factor  $R_k^A(x, Q^2)$  as

$$f_k^{\text{proton},A}(x, Q^2) = R_k^A(x, Q^2) f_k^{\text{proton}}(x, Q^2). \quad (6)$$

## 2.2 Experimental Input

The experimental data on which we base our analysis are differential charged-current neutrino\antineutrino-nucleus cross-sections<sup>3</sup>  $d^2\sigma^{\nu A, \bar{\nu} A}/dxdy$  measured at several values of neutrino beam energies  $E_\nu$ , Bjorken- $x$ , and virtuality  $Q^2$ . The NuTeV collaboration [15] provides 2618 and CDHSW [16] 1533 data points from Iron targets, whereas the CHORUS collaboration [17] gives 1214 data points from Lead target measurements. The kinematical reach of these data are illustrated by the polygons of Figure 1. The CTEQ analysis which is used here as reference for the proton PDFs imposes cuts in experimental data which will be also taken into account here. For consistency with this analysis and to avoid getting contaminated from higher-twist effects we restrict

---

<sup>2</sup>The EPS09-analysis was performed in the zero-mass scheme. However, in the presently studied region of  $x$ , we have checked that the difference between general-mass and zero-mass schemes in  $R_k^A(x, Q^2)$  are small.

<sup>3</sup>For a review of neutrino experiments, the reader can consult e.g. Ref. [23].

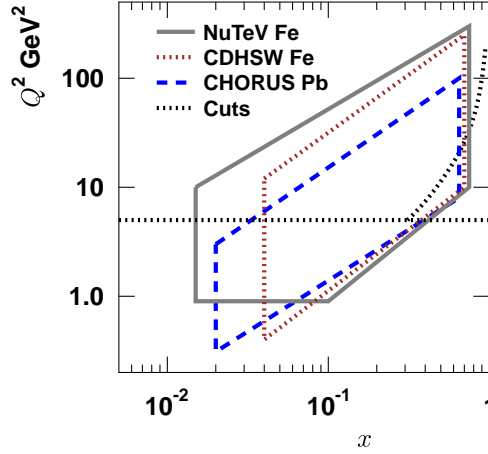


Figure 1: The kinematical reach of the NuTeV, CDHSW, and CHORUS neutrino data. The dotted black lines are the kinematical borderlines of Eq. (7).

the virtuality  $Q^2$  and the final state invariant mass  $W^2 = M^2 + Q^2(1-x)/x$  by the kinematical boundaries

$$Q_{\text{cut}}^2 > 5 \text{ GeV}^2, \quad W_{\text{cut}}^2 > 12 \text{ GeV}^2. \quad (7)$$

These cuts are indicated by black dotted lines in Figure 1. After applying these restrictions, 2041 NuTeV data points, 700 CDHSW, and 768 CHORUS data points remain.

## 2.3 Target Mass and Radiative Corrections

The two main types of additional correction factors that should be applied before a meaningful comparison to the experimental data are the target mass correction, and the one originating from the electroweak radiation.

The target mass corrections are important at large  $x$  and low  $Q^2$ . In this work, we apply the collinear factorization prescription from Ref. [24], which basically amounts to changing the Bjorken- $x$  variable to the Nachtmann variable, defined as  $\xi \equiv 2x/(1 + \sqrt{1 + 4x^2 M^2/Q^2})$ . To be precise, we make the substitution

$$\int_x^1 \frac{dz}{z} \omega_{ik}(z) f_k^A\left(\frac{x}{z}\right) \rightarrow \int_x^1 \frac{dz}{z} \omega_{ik}(z) f_k^A\left(\frac{\xi}{z}\right) \quad (8)$$

for the subprocesses involving light partons.

In contrast to the target mass corrections, the radiative corrections are rather a small- $x$  issue and more spread out in  $Q^2$ . To account for the radiative corrections, we use the parton flavor dependent factors  $\Delta_k^{\text{radiative}}$  from Ref. [25] correcting the leading

order terms, i.e. we compute

$$F_i^A = \sum_k [\omega_{ik}^{\text{LO}} (1 + \Delta_k^{\text{radiative}}) + \omega_{ik}^{\text{NLO}}] \otimes f_k^A. \quad (9)$$

Both corrections modify the  $Q^2$ -dependence of the calculated cross-sections. In the next sections, we will study the  $Q^2$ -dependence of the data vs. theory ratios and by examining them, one can judge whether obvious additional ingredients outside pQCD remain — only those regions of phase space where such behaviour is not evident, can be reliably used to make conclusions about the nuclear PDFs.

## 2.4 Probed PDF Components

To get a rough understanding of the behaviour of the neutrino cross-sections and their sensitivity to the different PDF-components, it is sufficient to consider the leading order expressions for the structure functions. For simplicity, we suppress the Cabibbo-Kobayashi-Maskawa matrix elements and assume that one is at large enough  $Q^2$  to forget about the heavy quark mass effects. Then, for the neutrino scattering

$$F_2^{\nu A} = 2x F_1^{\nu A} = 2x (d^A + s^A + b^A + \bar{u}^A + \bar{c}^A) \quad (10)$$

$$F_3^{\nu A} = 2 (d^A + s^A + b^A - \bar{u}^A - \bar{c}^A), \quad (11)$$

where e.g.

$$\begin{aligned} d^A &= \frac{Z}{A} d^{\text{proton},A} + \frac{A-Z}{A} d^{\text{neutron},A} \\ &= \frac{Z}{A} d^{\text{proton},A} + \frac{A-Z}{A} u^{\text{proton},A}, \end{aligned} \quad (12)$$

assuming the isospin symmetry. For the antineutrino scattering

$$F_2^{\bar{\nu}A} = 2x F_1^{\bar{\nu}A} = 2x (u^A + c^A + \bar{d}^A + \bar{s}^A + \bar{b}^A) \quad (13)$$

$$F_3^{\bar{\nu}A} = 2 (u^A + c^A - \bar{d}^A - \bar{s}^A - \bar{b}^A). \quad (14)$$

By inserting in Eq. (2), one finds that the cross-sections depend on the following partonic combinations:

$$d^2 \sigma^{\nu A} \propto (d^A + s^A + b^A) + (1-y)^2 (\bar{u}^A + \bar{c}^A) \quad (15)$$

$$d^2 \sigma^{\bar{\nu}A} \propto (\bar{d}^A + \bar{s}^A + \bar{b}^A) + (1-y)^2 (u^A + c^A). \quad (16)$$

Because of the suppressing  $(1-y)^2$  factor, the antineutrino cross-section carries more sensitivity to the sea quarks towards larger  $Q^2$ , whereas the neutrino cross-sections always get a significant contribution from the valence quarks.

## 2.5 The Method Of Comparison

In what follows, we will present the comparison to the data in terms of the following data vs. theory ratios:

$$R^{\text{CTEQ6.6}} \equiv \frac{\sigma^{\nu,\bar{\nu}}(\text{Experimental})}{\sigma^{\nu,\bar{\nu}}(\text{CTEQ6.6})}, \quad (17)$$

where CTEQ6.6 denotes the set of PDF used in the calculation. The PDF uncertainties are considered by calculating the upper and the lower cross-section uncertainties  $\Delta\sigma^\pm$  by a formula

$$(\Delta\sigma^\pm)^2 = \sum_k \left[ \max_{\min} \{ \sigma(S_k^+) - \sigma(S^0), \sigma(S_k^-) - \sigma(S^0), 0 \} \right]^2, \quad (18)$$

where  $\sigma(S^0)$  is the value of the cross-section computed by the CTEQ6.6 central set, and  $\sigma(S_k^\pm)$  are the ones calculated by the  $k$ th uncertainty sets. We will compare such “pseudodata” to the expected nuclear effects using the nuclear modification factors  $R_k^A(x, Q^2)$  from EPS09-analysis

$$R^{\text{CTEQ6.6} \times \text{EPS09}} \equiv \frac{\sigma^{\nu,\bar{\nu}}(\text{CTEQ6.6} \times \text{EPS09})}{\sigma^{\nu,\bar{\nu}}(\text{CTEQ6.6})}, \quad (19)$$

which allow us to make a conclusion about the consistency of the nuclear effects between neutrino scattering and the charged lepton scattering. We note that the EPS09 includes a possibility for a similar uncertainty analysis as in Eq. (18). The size of the uncertainties of this origin will be addressed in section 3.3.

## 3 Results and Discussion

### 3.1 The $\chi^2$ -values

The standard way of measuring the agreement between the experimental data and the theory, is to calculate the  $\chi^2$  defined as

$$\chi^2 \equiv \sum_{i \in \text{data points}} \left( \frac{T_i - D_i}{\sigma_i} \right)^2, \quad (20)$$

where  $T_i$  is the theoretical value, and  $D_i$  is the corresponding experimental value for the  $i$ th data point with estimated uncertainty  $\sigma_i$ <sup>4</sup>. In this work we add the statistical and systematic uncertainties in quadrature when computing  $\chi^2$ . Usually, if the  $\chi^2/N$  ( $N$  being the number of data points) is not much larger than one, the theoretical calculations are considered as being statistically consistent with the data.

---

<sup>4</sup>The experimental data used here have been taken from the database [26]. Statistical and systematic errors have been added in quadrature. Additional overall normalization errors have been ignored.

RAD + TM	CTEQ6.6	CTEQ6.6×EPS09
NuTeV	1.51	1.05
CHORUS	1.15	0.79
CDHSW	1.10	0.71
RAD + No TM	CTEQ6.6	CTEQ6.6×EPS09
NuTeV	1.29	1.02
CHORUS	1.03	0.85
CDHSW	0.88	0.66
No RAD + No TM	CTEQ6.6	CTEQ6.6×EPS09
NuTeV	1.35	1.08
CHORUS	1.23	1.09
CDHSW	0.96	0.86

Table 1: The  $\chi^2/N$ -values computed using CTEQ6.6 with and without nuclear modification from EPS09. The numbers are given for calculations including radiative and target mass correction (RAD + TM), with radiative but without target mass correction (RAD + No TM), and without radiative nor target mass corrections (No RAD + No TM).

In Table 1, we give the  $\chi^2/N$ -values, computed with those data points that meet our kinematical constraints. We have calculated the values in three different ways using CTEQ6.6 PDFs with and without nuclear modifications from EPS09: With the radiative and the target mass corrections, with the radiative but without target the mass correction, and finally without the radiative nor the target mass corrections. We make the following observations:

- Whatever way we make the calculation, the one without nuclear corrections from EPS09 gives substantially larger  $\chi^2$ .
- For CHORUS and CDHSW data, the  $\chi^2$ s get consistently smaller as the radiative and target mass are applied.
- For NuTeV data, the  $\chi^2$  remains practically unchanged whether radiative or target mass corrections are applied or not.

Whereas the good  $\chi^2/N$ -values indicate that the theory calculations are in good agreement with the data, it may seem puzzling that while  $\chi^2$ s for CHORUS and CDHSW gain improvement when applying the radiative and the target mass corrections, the  $\chi^2_{\text{NuTeV}}$  stays essentially constant.

The fact that the  $\chi^2_{\text{CHORUS}}$  and  $\chi^2_{\text{CDHSW}}$  get clearly smaller after addition of the radiative and target mass corrections indicates, that there are a substantial changes in the computed cross-sections. Therefore, the unchanging  $\chi^2_{\text{NuTeV}}$  implies that there is something peculiar in the NuTeV data sample.

We note that the target mass correction, Eq. (8), was not applied in the EPS09-analysis. Repeating the analysis including such effect would slightly change the shape



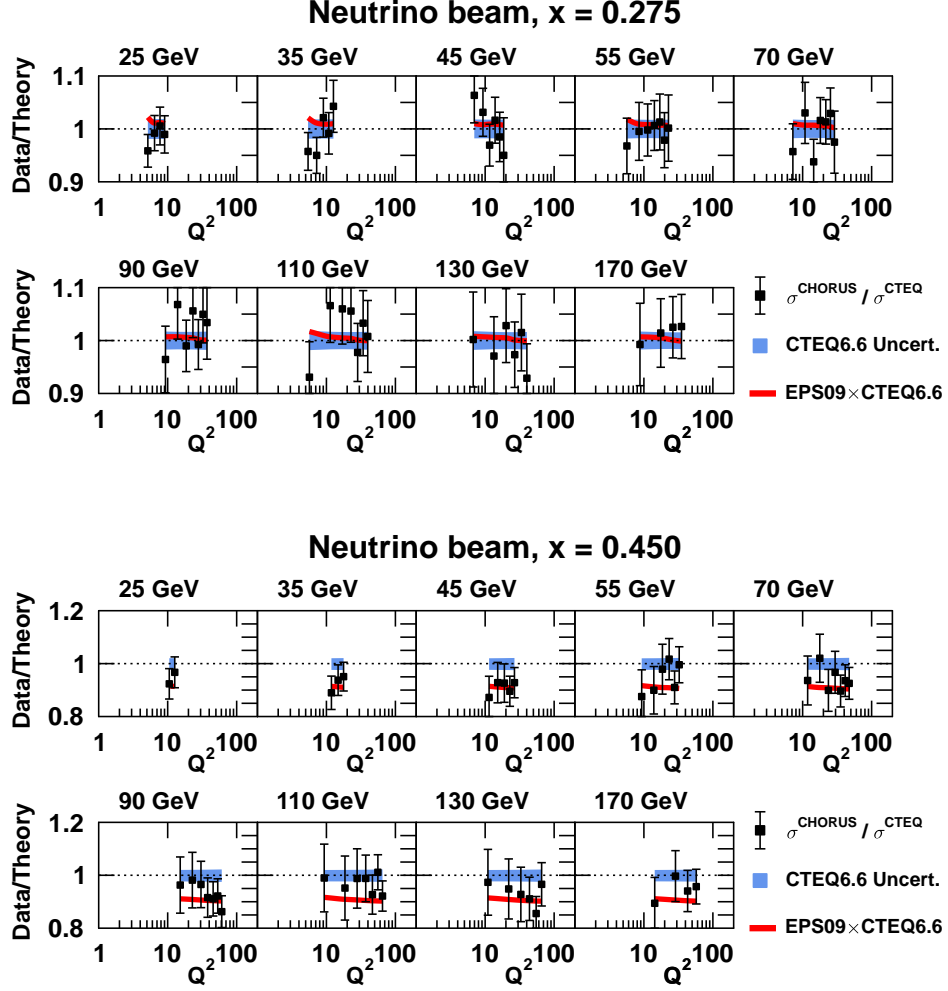


Figure 2: Examples of Data/Theory ratios for the CHORUS neutrino data. The black squares with error bars correspond to the ratios  $R^{\text{CTEQ6.6}}$ , whereas the red lines are the  $R^{\text{CTEQ6.6} \times \text{EPS09}}$  predictions. The relative CTEQ6.6 uncertainty is shown by blue bands.

of the valence quark nuclear modifications at large- $x$ . Moreover, the CTEQ6.6 uncertainties also grow towards large  $x$ . Both effects, if taken into account, would modify the  $\chi^2$  evaluation of the data in this region of phase space. Therefore, the changes in  $\chi^2$  when applying the target mass corrections for the CTEQ6.6  $\times$  EPS09 column of Table 1 should be taken only as indicative. Note, however, how the  $\chi^2$  gets clearly worse when adding the target mass correction if the nuclear PDFs are not used.

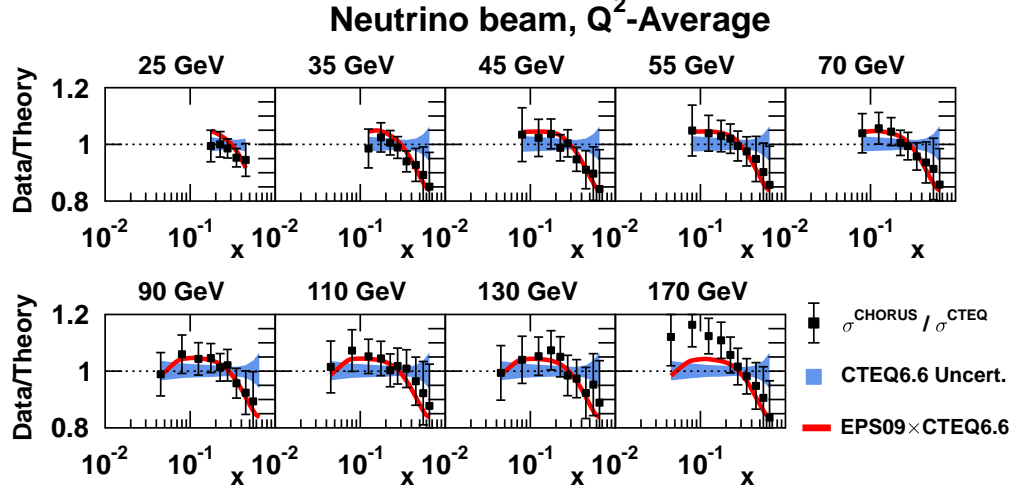


Figure 3: The  $Q^2$ -averaged CHORUS neutrino data. The black squares with errorbars show the  $R_{\text{Average}}^{\text{CTEQ6.6}}$  ratios, while the red lines correspond to  $R_{\text{Average}}^{\text{CTEQ6.6} \times \text{EPS09}}$ . The blue bands denote the average relative uncertainty in the cross-sections  $d^2\sigma^\nu(\text{CTEQ6.6})$ .

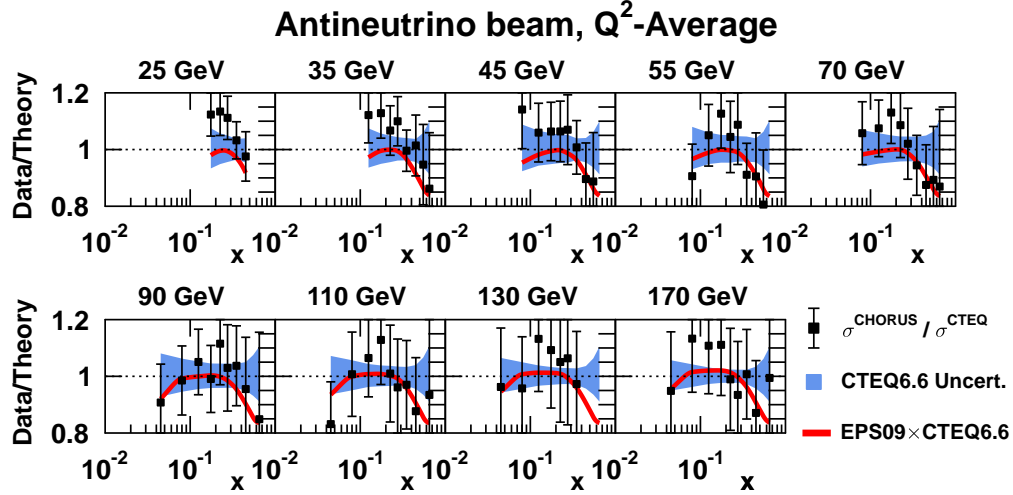


Figure 4: As Figure 3, but for CHORUS antineutrino data.

### 3.2 Data vs. Theory Ratios

In this section we take a closer look to the nuclear effects in neutrino-nucleus DIS by plotting results for ratios  $R^{\text{CTEQ6.6}}$  and  $R^{\text{CTEQ6.6} \times \text{EPS09}}$ . To begin with, the Figure 2 shows two representative examples of the energy and  $Q^2$ -dependence of the data vs. theory ratios. Evidently, as one cannot observe a large systematic  $Q^2$ -dependence in

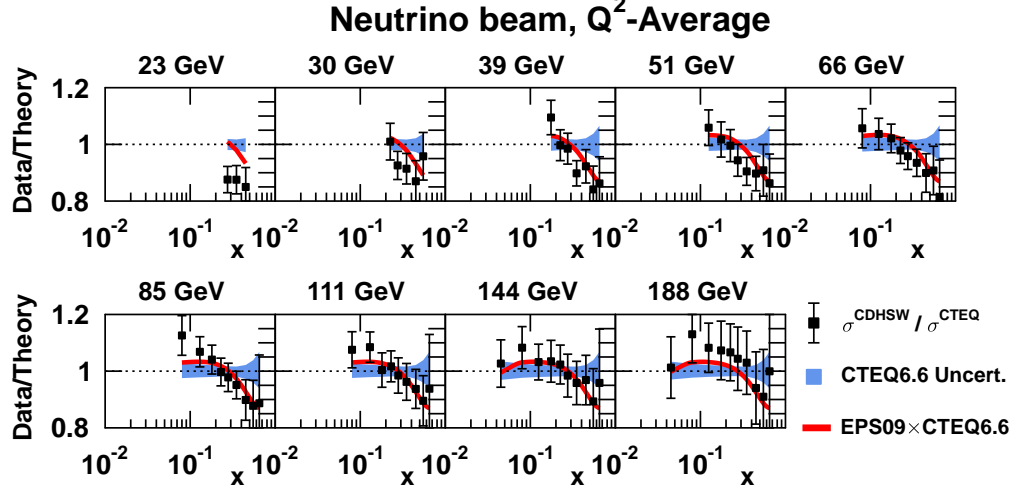


Figure 5: As Figure 3, but for CDHSW neutrino data.

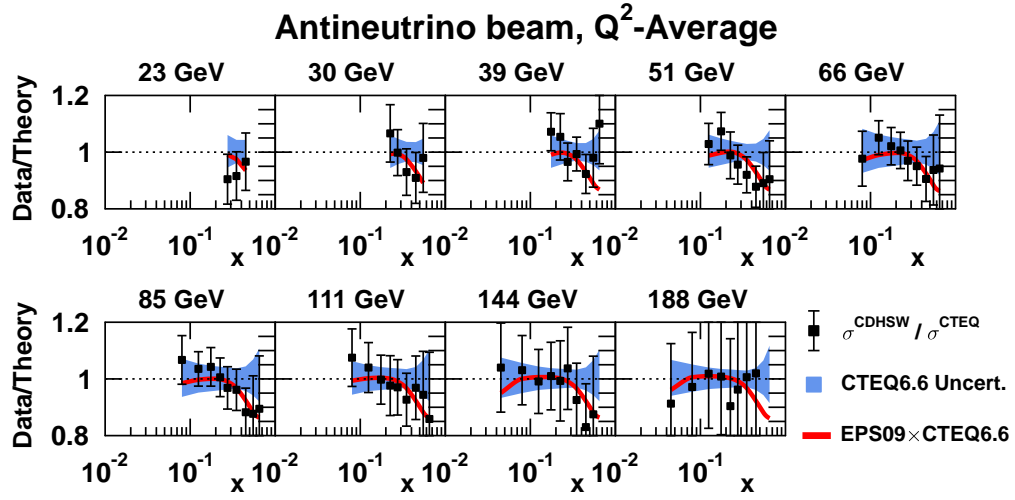


Figure 6: As Figure 3, but for CDHSW antineutrino data.

these panels, it is reasonable to look at  $Q^2$ -averaged versions of these figures in order to better see the big picture — the  $x$ -shape of the nuclear modifications.

We will form the  $Q^2$ -averages of the panels by the prescription

$$R_{\text{Average}}^{\text{CTEQ6.6}} \equiv \left( \sum_{i \in \text{fixed } x}^N \frac{R_i^{\text{CTEQ6.6}}}{\sigma_i} \right) \left( \sum_{i \in \text{fixed } x}^N \frac{1}{\sigma_i} \right)^{-1} \pm N \times \left( \sum_{i \in \text{fixed } x}^N \frac{1}{\sigma_i} \right)^{-1}, \quad (21)$$

where the sum runs over all data points in same  $x$ - and energy-bin, but different  $Q^2$ . We

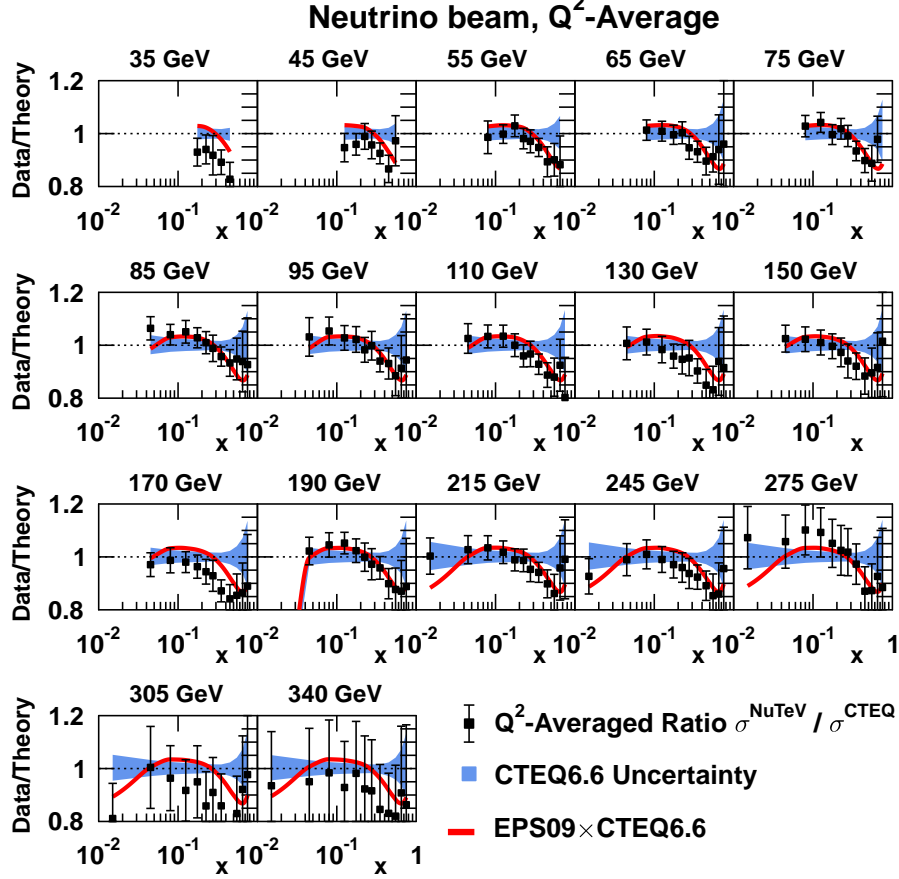


Figure 7: As Figure 3, but for NuTeV neutrino data.

note that the way we compute the average and, especially its uncertainty, is not meant to be statistically “the correct way”, but it is rather meant to give an idea about the size of the uncertainties. We stress, however, that the statistical analysis (the calculation of the  $\chi^2$ -values in the previous sections) was performed with the original (non-averaged) data. The purely theoretical calculations are simple averages, for example

$$R_{\text{Average}}^{\text{CTEQ6.6} \times \text{EPS09}} \equiv \frac{1}{N} \sum_{i \in \text{fixed } x}^N R_i^{\text{CTEQ6.6} \times \text{EPS09}}. \quad (22)$$

The results of this exercise are presented in Figures 3-8. We wish to draw the reader’s attention to the following points:

- The CTEQ6.6×EPS09-prediction and the CHORUS and CDHSW neutrino data are in a perfect agreement. The data do not display an evident dependence of the neutrino energy. This is also true for the CDHSW antineutrino data.

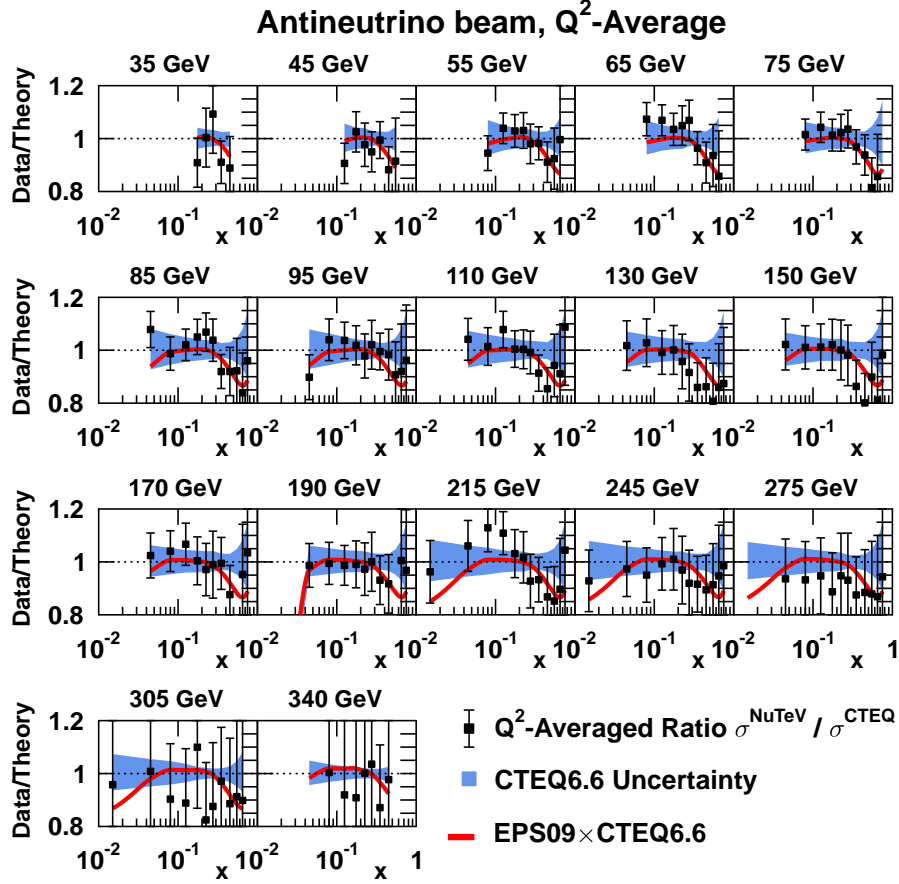


Figure 8: As Figure 3, but for NuTeV antineutrino data.

- The CHORUS antineutrino data seems to somewhat overshoot the CTEQ6.6 $\times$ EPS09-prediction around  $x \sim 0.2$  staying, however, clearly in the uncertainty limits.
- Whereas some panels corresponding to the NuTeV neutrino data are very well in line with the CTEQ6.6 $\times$ EPS09 prediction, there is an evident variation from a beam energy to another. For example  $E_\nu = 170$  GeV and  $E_\nu = 190$  GeV are in the brink of disagreement.
- Similar evident energy-dependence is not observable in the NuTeV antineutrino panels. Within the uncertainties the data are well reproduced.

The clear energy-dependent panel-to-another variation in the NuTeV neutrino data/theory ratios is evidently something that cannot be compensated by only re-fitting the PDFs — the CTEQ6.6 $\times$ EPS09 predictions vary very slowly as a function of the incident neutrino energy. On the contrary, using this data set as a source of PDFs in a fit would

inevitably result in a compromise between data in different energy bins displaying mutual tension. No signs of this kind of evident controversy are visible in the NuTeV antineutrino data nor in the CHORUS or CDHSW data.

This observation also explains why the  $\chi^2_{\text{NuTeV}}$  is almost inert to the target mass and radiative corrections. Indeed, by simply ignoring the  $E_\nu = 35, 45, 130, 150, 170, 245$  GeV panels when computing  $\chi^2_{\text{NuTeV}}$ , would cause the  $\chi^2_{\text{NuTeV}}/N$  to reduce from 1.10 to 0.94 when applying the corrections.

### 3.3 Other Sets of nPDFs

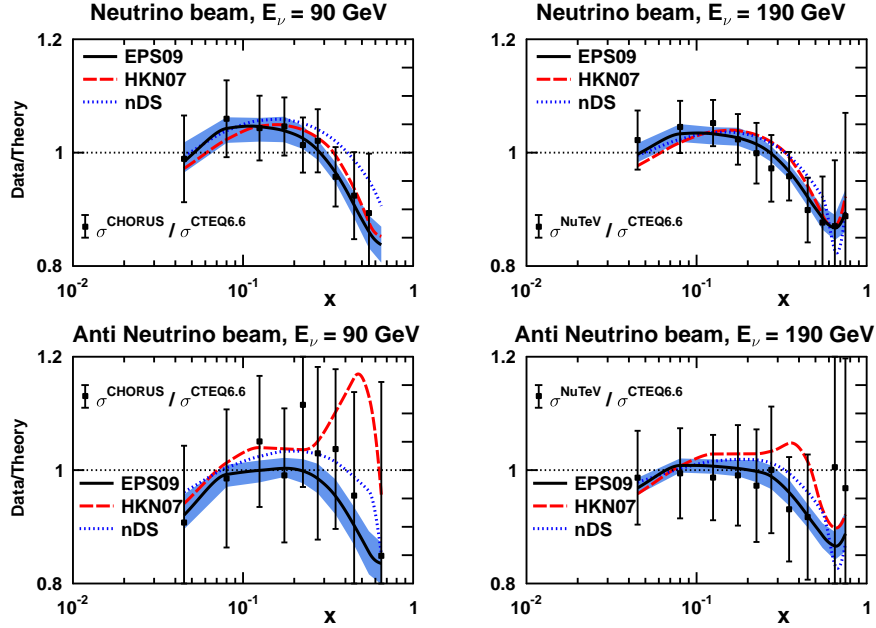


Figure 9: Two panels of  $Q^2$ -averaged CHORUS and NuTeV data with predictions from three sets of nPDFs, EPS09 (black line with blue errorband), HKN07 (red dashed line), and nDS (blue dotted line).

So far we have considered the nuclear effects in PDFs utilizing solely the latest available analysis, EPS09, observing a good average agreement with the experimental data. To address whether the same conclusion would have been drawn using different sets of nPDFs we show, in Figure 9, examples of the  $Q^2$ -averaged ratios from the two other available NLO sets nDS and HKN07, and compare them to the uncertainty band of EPS09.

The upper panels illustrate the situation with the neutrino cross-sections. At large  $x$ , the dominant contribution to the cross-sections comes from the valence quarks and — due to good amount of valence quark constrains from charged lepton DIS there — the different sets of nPDFs give predictions relatively close to each other. Only the

nDS prediction for Lead display a clear deviation from others. Towards small  $x$ , the predictions from different sets of nPDFs are very close to each other.

In the case of antineutrino cross-sections, illustrated in the lower panels, there is an enhanced contribution from the sea quarks, for which the nuclear modifications at large  $x$  are not very well constrained. This uncertainty is reflected as clearly larger scatter between the curves. At small  $x$ , all sets of nPDFs are again in a good agreement.

In summary, it is mainly in the large- $x$  sector where the differences between sets of nPDFs become apparent: While the nDS description admits some improvements especially regarding the  $A$ -dependence in this region, the HKN07, on the other hand clearly misses the structure of antineutrino cross-sections at large- $x$ . This is due to the radically different behavior of antiquarks and gluons when compared with the two other sets in the corresponding relevant region of phase space. These findings point also to the adequacy of neutrino data in providing further constraints for nPDFs.

## 4 Conclusion

In this article we have presented a study of the nuclear effects in the (anti)neutrino-nucleus deeply inelastic scattering. As a conclusion, we find that from the analysed data sets only one — the NuTeV neutrino data — shows signs of not being in a complete agreement with the present-day PDFs. This discrepancy, we argue, is however something that cannot be completely cured by simply re-fitting the PDFs. Rather, it is due to an unexplained, neutrino energy-dependent fluctuations in the data — in order to make this point more explicit, we have presented  $Q^2$ -averaged data where the energy systematics of the  $x$ -dependence is more transparent. Therefore we assert that this data set cannot be taken as a discriminating factor when making conclusions about universality of the nuclear PDFs. The forthcoming data from NOMAD experiment will eventually facilitate a further clarification about the conflict between the different experiments.

Apart from this finding, the present analysis do not give any reason to believe that the nuclear effects in neutrino-nucleus DIS would be different from those extracted from charged lepton DIS and DY production of dileptons — the factorization seems to work well.

Having said that, there is a lot of room for improvement and future work. For example, the EPS09-analysis leaves no freedom to the strange quark nuclear modification, but it is something that is fixed by hand to other sea quarks. As the antineutrino cross-sections carry a non-negligible contribution from the strange quarks, including these data to a global fit of nPDFs would offer a chance to free this assumption made in EPS09. This could improve the slight undershooting of the CHORUS antineutrino data. Also, whereas the Iron is almost an isoscalar nucleus ( $Z = 26$ ,  $N = 30$ ), the Lead is clearly non-isoscalar ( $Z = 82$ ,  $N = 126$ ). This could offer a possibility to separately constrain the nuclear modifications for the up and down quarks which has not been possible before.

## Acknowledgments

We thank Néstor Armesto for useful discussions. This work is supported by Ministerio de Ciencia e Innovación of Spain under project FPA2009-06867-E; by Xunta de Galicia (Consellería de Educación and Consellería de Innovación e Industria – Programa Incite); by the Spanish Consolider-Ingenio 2010 Programme CPAN (CSD2007-00042); and by the European Commission grant PERG02-GA-2007-224770. CAS is a Ramón y Cajal researcher.

## References

- [1] P. M. Nadolsky *et al.*, Phys. Rev. D **78** (2008) 013004 [arXiv:0802.0007 [hep-ph]].
- [2] A. D. Martin, W. J. Stirling, R. S. Thorne and G. Watt, Eur. Phys. J. C **63** (2009) 189 [arXiv:0901.0002 [hep-ph]].
- [3] R. D. Ball, L. Del Debbio, S. Forte, A. Guffanti, J. I. Latorre, J. Rojo and M. Ubiali, arXiv:1002.4407 [hep-ph].
- [4] Y. L. Dokshitzer, Perturbation Theory In Quantum Sov. Phys. JETP **46** (1977) 641 [Zh. Eksp. Teor. Fiz. **73** (1977) 1216]; V. N. Gribov and L. N. Lipatov, Yad. Fiz. **15** (1972) 781 [Sov. J. Nucl. Phys. **15** (1972) 438]; V. N. Gribov and L. N. Lipatov, Yad. Fiz. **15** (1972) 1218 [Sov. J. Nucl. Phys. **15** (1972) 675]; G. Altarelli and G. Parisi, Nucl. Phys. B **126** (1977) 298.
- [5] K. J. Eskola, H. Paukkunen and C. A. Salgado, JHEP **0904** (2009) 065 [arXiv:0902.4154 [hep-ph]].
- [6] I. Schienbein, J. Y. Yu, K. Kovarik, C. Keppel, J. G. Morfin, F. Olness and J. F. Owens, Phys. Rev. D **80** (2009) 094004 [arXiv:0907.2357 [hep-ph]].
- [7] M. Hirai, S. Kumano and T. H. Nagai, arXiv:0709.3038 [hep-ph].
- [8] D. de Florian and R. Sassot, Phys. Rev. D **69** (2004) 074028 [arXiv:hep-ph/0311227].
- [9] K. J. Eskola, H. Paukkunen and C. A. Salgado, JHEP **0807** (2008) 102 [arXiv:0802.0139 [hep-ph]].
- [10] M. Hirai, S. Kumano and T. H. Nagai, Phys. Rev. D **71** (2005) 113007 [arXiv:hep-ph/0412284].
- [11] K. J. Eskola and H. Paukkunen, JHEP **0606** (2006) 008 [arXiv:hep-ph/0603155].
- [12] S. A. Kulagin and R. Petti, Phys. Rev. D **76** (2007) 094023 [arXiv:hep-ph/0703033].



- [13] N. Armesto, C. Merino, G. Parente and E. Zas, Phys. Rev. D **77** (2008) 013001 [arXiv:0709.4461 [hep-ph]].
- [14] I. Schienbein, J. Y. Yu, C. Keppel, J. G. Morfin, F. Olness and J. F. Owens, Phys. Rev. D **77** (2008) 054013 [arXiv:0710.4897 [hep-ph]].
- [15] M. Tzanov *et al.* [NuTeV Collaboration], Phys. Rev. D **74** (2006) 012008 [arXiv:hep-ex/0509010].
- [16] J. P. Berge *et al.*, Z. Phys. C **49** (1991) 187.
- [17] G. Onengut *et al.* [CHORUS Collaboration], Phys. Lett. B **632** (2006) 65.
- [18] M. A. G. Aivazis, F. I. Olness and W. K. Tung, Phys. Rev. D **50** (1994) 3085 [arXiv:hep-ph/9312318].
- [19] M. A. G. Aivazis, J. C. Collins, F. I. Olness and W. K. Tung, Phys. Rev. D **50** (1994) 3102 [arXiv:hep-ph/9312319].
- [20] M. 1. Kramer, F. I. Olness and D. E. Soper, Phys. Rev. D **62** (2000) 096007 [arXiv:hep-ph/0003035].
- [21] S. Kretzer, H. L. Lai, F. I. Olness and W. K. Tung, Phys. Rev. D **69** (2004) 114005 [arXiv:hep-ph/0307022].
- [22] W. K. Tung, H. L. Lai, A. Belyaev, J. Pumplin, D. Stump and C. P. Yuan, JHEP **0702** (2007) 053 [arXiv:hep-ph/0611254].
- [23] J. M. Conrad, M. H. Shaevitz and T. Bolton, Rev. Mod. Phys. **70** (1998) 1341 [arXiv:hep-ex/9707015].
- [24] A. Accardi and J. W. Qiu, JHEP **0807** (2008) 090 [arXiv:0805.1496 [hep-ph]].
- [25] A. B. Arbuzov, D. Y. Bardin and L. V. Kalinovskaya, JHEP **0506** (2005) 078 [arXiv:hep-ph/0407203].
- [26] <http://durpdg.dur.ac.uk/HEPDATA/>